



Published in final edited form as:

Oncogene. 2014 February 20; 33(8): 977–985. doi:10.1038/onc.2013.39.

Constitutively active TrkB confers an aggressive transformed phenotype to a neural crest derived cell line

John DeWitt, MS¹, Vanessa Ochoa, BS¹, Johann Urschitz, PhD², Marlee Elston, BS², Stefan Moisyadi, PhD², and Rae Nishi, PhD^{1,*}

¹Dept. Anatomy and Neurobiology and Neuroscience Graduate Program, University of Vermont, 149 Beaumont Ave, Burlington, VT 05405

²Dept. Anatomy, Biochemistry, and Physiology, John A Burns School of Medicine, Honolulu, HI 96822

Abstract

Neuroblastoma arises from sympathoadrenal progenitors of the neural crest and expression of the neurotrophin receptor TrkB and its ligand, brain-derived neurotrophic factor (BDNF) is correlated with poor prognosis. Although activated TrkB signaling promotes a more aggressive phenotype in established neuroblastoma cell lines, whether TrkB signaling is sufficient to transform neural crest derived cells has not been investigated. To address the role of TrkB signaling in malignant transformation, we removed two immunoglobulin-like domains from the extracellular domain of the full length rat TrkB receptor to create a IgTrkB that is constitutively active. In the pheochromocytoma-derived cell line PC12, IgTrkB promotes differentiation by stimulating process outgrowth; however, in the rat neural crest derived cell line NCM-1, IgTrkB signaling produces a markedly transformed phenotype characterized by increased proliferation, anchorage-independent cell growth, anoikis resistance, and matrix invasion. Furthermore, expression of IgTrkB leads to up-regulation of many transcripts encoding cancer-associated genes including *cyclind1*, *twist1*, and *hgf*, as well as down-regulation of tumor suppressors such as *pten*, and *rb1*. In addition, IgTrkB NCM-1 cells show a 21-fold increase in mRNA for MYCN, the most common genetic marker for a poor prognosis in neuroblastoma. When injected into NOD SCID mice, control GFP NCM-1 cells fail to grow while IgTrkB NCM-1 cells form rapidly growing and invasive tumors necessitating euthanasia of all mice by 15 days post injection. In summary, these results indicate that activated TrkB signaling is sufficient to promote the formation of a highly malignant phenotype in neural crest derived cells.

Keywords

Neuroblastoma; neural crest; transformation; TrkB; MYCN

Users may view, print, copy, download and text and data- mine the content in such documents, for the purposes of academic research, subject always to the full Conditions of use: http://www.nature.com/authors/editorial_policies/license.html#terms

*Corresponding Author: Rae Nishi, HSRF 406, 149 Beaumont Ave., Burlington, VT 05405, Telephone: (802) 656-4504, Fax: (802) 656-8704, Rae.Nishi@med.uvm.edu.

Conflict of interest

The authors declare no conflict of interest.

Supplementary information is available at the *Oncogene* website (<http://www.nature.com/onc>)

Introduction

Neuroblastoma, a pediatric malignancy arising from sympathoadrenal precursors from the neural crest, is a cancer typified by its heterogeneity of disease. Disease course in neuroblastoma can range anywhere from patients presenting with metastatic disease that will spontaneously regress with support treatment alone (stage 4S), to localized favorable tumors, to cases of aggressive neuroblastoma, in which children will often relapse following treatment despite the most intensive chemo- and adjuvant therapy (1).

This heterogeneity in neuroblastoma tumor properties is correlated with a number of different factors including Trk receptor expression (2). Trk receptors are important in normal sympathetic development; for example, TrkA, the high affinity receptor for nerve growth factor (NGF), promotes target-dependent survival of sympathetic neurons by preventing programmed cell death (3, 4) and neuroblastoma tumors that express TrkA have a favorable prognosis (5). In contrast, many MYCN amplified, poor prognosis neuroblastomas express TrkB, resulting in tumors that are often highly aggressive and eventually fatal (6). Because TrkB promotes plasticity, differentiation and survival of primary neurons, the aggressive phenotype correlated with TrkB expression was puzzling; however, we discovered that TrkB is transiently expressed in sympathetic progenitors prior to the onset of TrkA expression, and when stimulated with BDNF, the TrkB expressing cells proliferate in cell culture (7, 8) and in vivo (Straub and Nishi, unpublished observations).

An important question is whether TrkB expression is a marker of poor prognosis, or whether active TrkB signaling is directly responsible for the aggressive nature of poor prognosis neuroblastoma. Supporting a causal role for TrkB signaling, concomitant expression of full length TrkB and BDNF leads to autocrine signaling enhancing tumor cell survival and invasiveness (9), while expression of a truncated TrkB isoform lacking the tyrosine kinase domain is commonly found in more benign and differentiated tumors such as ganglioneuroblastomas (10). Furthermore, treatment of TrkB-expressing SMS-KCN neuroblastoma cells with BDNF enhances cell survival in serum free media (11). Similarly BDNF treatment of SH-SY5Y cells either transfected with TrkB or induced to express TrkB by retinoic acid have enhanced survival in conditions of limited growth factors (9, 12), increased resistance to chemotherapeutics (13–15), increased production of angiogenic factors (16, 17), and enhanced invasion (9). Therefore, TrkB signaling contributes to the aggressiveness of poor prognosis neuroblastoma, but it is still unknown whether TrkB signaling alone can transform cells of the neural crest lineage.

In order to determine if constitutively active TrkB signaling is sufficient to transform cells, we created a mutant form of the TrkB receptor by removal of two immunoglobulin-like ligand binding domains in the extracellular portion of the receptor. This construct is constitutively active and, when stably transfected into a normal neural crest-derived cell line NCM-1, promotes a highly malignant phenotype in vitro and in vivo.

Results

Removal of two immunoglobulin-like domains renders TrkB constitutively active

Previous studies have shown the TrkA tyrosine kinase receptor can be rendered constitutively active by removal of the two immunoglobulin-like (Ig-like) domains in the extracellular region of the receptor (18). Therefore, we created a similar construct (IgTrkB; Figure S1) and stably transfected HEK293 cells with IgTrkB and full length wild type (WT) TrkB. Expression of both types of receptor were confirmed (Figure 1a). A marked increase of phosphorylated Erk 1/2 is observed when WT TrkB HEK293 cells are treated with BDNF and IgTrkB HEK293 cells (Figure 1a) albeit at significantly lower levels when compared to the BDNF-stimulated WT TrkB (Figure 1b). Therefore, we tested whether this level of constitutive signaling by IgTrkB was sufficient to promote downstream biological effects.

IgTrkB promotes neurite outgrowth in PC12 cells

PC12 cells are a well-known model of nerve growth factor (NGF) induced neuronal differentiation via TrkA (19, 20), and TrkB transfected PC12 cells differentiate in response to BDNF (21). PC12 cells were transiently transfected with IgTrkB or GFP control construct, and two days later treated with or without 7sNGF (1µg/mL). After 6 days, cells were fixed and stained for either TrkB or GFP to identify transfected cells. Cells transfected with IgTrkB show a 6-fold increase in the number of neurite bearing cells over GFP transfected cells in the absence of NGF (Figure 2a–c). The IgTrkB-induced neurite outgrowth is equivalent to that of NGF through TrkA as there is no difference in the number of neurite bearing cells between IgTrkB or GFP transfected cells in the presence of NGF (Figure 2d).

IgTrkB enhances proliferation in the neural crest derived cell line NCM-1

NCM-1 is an immortalized, but normal multipotent cell line with the ability to generate sympathoadrenal precursors (22). To determine if constitutive TrkB signaling promotes proliferation or differentiation in NCM-1 cells, we transfected cells with IgTrkB using a PiggyBac transposase/transposon vector (pmGenie 3) that integrates the desired insert into the host chromosome followed by inactivation of the transposase (23). Stable IgTrkB NCM-1 transfectants grow to confluency more rapidly than untransfect (CONT) NCM-1 cells. To quantify this apparent increase in proliferation, cells were counted after various times in cell culture by measuring uptake of the vital fluorescent dye calcein AM (24). We noted a 2.5-fold increase in cell number after 4 days in IgTrkB NCM-1 cells compared to CONT NCM-1 cells (Figure 3a). While constitutively active TrkA is transforming, full length (WT) TrkA plus NGF promotes differentiation (25); therefore, we compared the growth rate of WT TrkB NCM-1 cells with or without BDNF. As seen in Figure 3b, the growth rate of WT TrkB NCM-1 cells is enhanced by the presence of BDNF. Thus, ligand induced activation of WT TrkB also enhances proliferation as does the IgTrkB. Additionally, treatment with the pan-Trk kinase inhibitor K252a abolished IgTrkB-mediated proliferation, resulting in calcein AM fluorescence equivalent to CONT NCM-1 cells (Figure 3c) suggesting that TrkB kinase activity is required for the observed enhanced proliferation. In order to confirm that the enhanced proliferation did not arise from an

insertion of our construct into a tumor suppressor, five additional parent lines were established that all show a significant increase in cell number after 4 days in vitro (Figure S2). Further supporting the enhanced proliferation, western blot analysis for the proliferation markers, phosphorylated histone H3 and cyclin D1 kinase show significant increases in IgTrkB NCM-1 compared to CONT NCM-1 cells (Figure S3). Therefore, constitutive signaling through IgTrkB promotes an enhanced rate of growth in CONT NCM-1 cells.

IgTrkB transforms NCM-1 cells

Enhanced proliferation alone is not sufficient to consider a cell transformed. Another feature common to transformed cells is the loss of requirement for attachment to a surface to divide, a property known as anchorage independent cell growth (26). To determine if IgTrkB expression confers anchorage independent cell growth to NCM-1 cells, cells were cultured suspended in soft agar (Figure 4). While CONT NCM-1 cells failed to grow colonies in soft agar regardless of the presence of BDNF (Figure a,b), IgTrkB NCM-1 cells grow many colonies whether or not BDNF is present (Figure 4c,d,g). In contrast very few colonies are formed by WT TrkB cells in the absence of BDNF (Figure 4e,g) but many are formed when WT TrkB NCM-1 cells are stimulated by BDNF (Figure 4f,g). Interestingly the number of colonies formed mirrored the level of phospho-ERK activation (compare Figure 1b to 4g). Furthermore, although IgTrkB NCM-1 cells formed fewer colonies, the colonies that formed appeared larger than those formed by WT TrkB in the presence of BDNF (compare Figure 4d to 4f).

Another feature related to anchorage independent growth is the ability of transformed cells to survive when detached from the cell surface (27). Normally, when cells grown in culture detach, they undergo anoikis, or detachment induced apoptosis. To determine if IgTrkB allows NCM-1 cells to become anoikis resistant, the number of live cells in the medium collected from transfected and untransfected cells was quantified (Figure 4h). We observed a 4-fold increase in the number of live cells in the media from IgTrkB NCM-1 cultures compared to CONT NCM-1 ($p < 0.05$, Figure 4d), indicating IgTrkB promotes anoikis resistance in NCM-1 cells.

Another important characteristic of malignant transformation is the ability of cells to migrate to and invade surrounding tissues and blood vessels. To investigate whether IgTrkB expression enhances migration and invasion we used a radial migration assay known as ‘the donut assay’ (28). In this assay, cells are limited to a restricted area by a silicone donut. Following donut removal, the number of cells migrating radially from the confined area are quantified. Neural crest cells are intrinsically migratory, as during development they must migrate from the neural tube to their final locations throughout the body. In light of this, we did not find any significant difference in the total number of migrating cells outside the originally confined area after 24 hours (Figure 5a–c, e–g, j). However, there is a significant increase in the area within which migrated cells could be found, indicating IgTrkB NCM-1 cells migrate farther compared to WT NCM-1 cells (Figure 5d, h–i).

To investigate invasion, a layer of crude extracellular matrix (matrigel) was overlaid on the cells. Although addition of matrigel leads to a reduction in the number of cells traveling outside the originally confined area for both cell types (Figure 5j vs. 5t), IgTrkB NCM-1

cells have an enhanced ability to invade the extracellular matrix marked by a 2.5-fold increase in the number of cells invading after 24 hours (Figure 5k–m, o–q, t). Furthermore, IgTrkB NCM-1 cells invade farther into the matrigel indicated by a 2.5-fold increase in the total area invaded by IgTrkB NCM-1 cells compared to CONT NCM-1 (Figure 5n, r, s).

IgTrkB enhances cancer related gene expression in NCM-1 cells

To identify genes contributing to the transformed phenotype in IgTrkB NCM-1 cells, we analyzed transcripts using a targeted qPCR array of cancer pathway genes (full table of genes analyzed is in the Supplemental Materials). This analysis revealed that IgTrkB increases transcript levels for a number of tumor promoting genes (Table 1), as well as decreases in expression of tumor suppressors (Table 2). Consistent with the enhanced proliferation of IgTrkB NCM-1 cells, we detected a 436-fold increase in transcripts levels as well as significantly enhanced protein levels (Figure S3) for the cell cycle regulatory gene *cyclind1*. Furthermore, upregulation of *twist1* (39-fold) and hepatocyte growth factor (*hgf*, 29-fold), two genes known to play important roles in promoting invasion and metastasis (29, 30), is consistent with the enhanced invasive capacity of IgTrkB NCM-1 cells. Moreover, expression of IgTrkB in NCM-1 cells significantly downregulates expression of the tumor suppressors *pten* (-1.71-fold) and *rb1* (-1.77-fold). Therefore, the RNA expression profile of IgTrkB NCM-1 cells is consistent with the highly transformed phenotype of the cells.

An important marker of poor prognosis in human neuroblastoma tumors is the amplified expression of *mycn*. To determine if the transformation of NCM-1 cells by IgTrkB influences *mycn*, we compared transcript levels in CONT and IgTrkB NCM-1 cells by qPCR. We found a 21-fold increase in *mycn* levels in IgTrkB NCM-1 cells compared to CONT NCM-1 cells ($p < 0.01$). In contrast, although NCM-1 cells were immortalized by the use of a retroviral vector carrying *vmyc*, the levels of *myc* observed with the qPCR array were very low and did not differ between CONT- and IgTrkB NCM-1 cells (see supplemental material regarding the gene list and qPCR array signals observed for each gene).

IgTrkB NCM-1 cells form rapidly growing and aggressive tumors in vivo

To determine if IgTrkB expression would enhance the ability of NCM-1 cells to form tumors in vivo, NOD-SCID mice were injected subcutaneously with 10^6 IgTrkB or GFP NCM-1 cells suspended in matrigel. One week following injection, tumors became palpable in mice injected with IgTrkB NCM-1 cells (Figure 6a, $p < 0.01$), and all IgTrkB NCM-1 injected mice were sacrificed by 15 days post-injection due to tumor burden (Figure 6b). GFP NCM-1 injected mice remained tumor free throughout the experiment (Figure 6). Monitoring tumor size daily, IgTrkB NCM-1 tumors grew extremely rapidly, measuring an estimated 8 cm³ by 2 weeks after injection, while GFP NCM-1 cells failed to grow (Figure 6c). Upon removal, IgTrkB NCM-1 cell tumors were extremely large and heavily vascularized with an average wet weight of 4.5 grams (Figure 6e–f). Not only do IgTrkB tumors grow at a rapid pace, these tumors are also highly invasive, invading the vertebrae and compressing the spine resulting in bilateral hind limb paralysis in one mouse only 10 days following injection (Figure 6g–h). Tumor tissue contains many closely packed cells with scant cytoplasm and little extracellular stroma, reminiscent of aggressive, poor

prognosis neuroblastoma (Figure 6d). Furthermore, a separate injection of only 100 cells formed tumors in 3/3 mice within 21 days, demonstrating IgTrkB NCM-1 cells are highly tumorigenic. Therefore, constitutive TrkB signaling is sufficient to transform the neural crest derived cell line NCM-1 into highly aggressive tumor cells in vivo.

Discussion

In this study we provide evidence that constitutive TrkB signaling is sufficient to transform a neural crest cell line into a carcinogenic phenotype marked by an enhancement of proliferation, anchorage independent cell growth, anoikis resistance, migration and invasion, and upregulation of tumor promoter genes. The enhanced rate of proliferation and anchorage independent cell growth was also observed when full length TrkB was stimulated with BDNF in the same cell line. The isolation of the IgTrkB NCM-1 cell line allowed us to test the behavior of these cells in vivo, and they displayed highly aggressive, tumorigenic behavior when injected subcutaneously. Taken together, our data suggest that aberrant TrkB signaling in the developing sympathoadrenal lineage may be sufficient to promote neuroblastoma formation.

The involvement of Trk receptors in cancer is complex. The first Trk, for “tropomyosin-receptor kinase”, was isolated from a colon carcinoma, and resulted from the fusion of a truncated tropomyosin with the tyrosine kinase domain of a receptor that rendered the kinase constitutively active (31). This kinase domain was subsequently discovered to belong to TrkA, the high affinity receptor for nerve growth factor (NGF; (20). In neuroblastomas, activation of full length TrkA slows the rate of proliferation and promotes differentiation, and shorter forms of TrkA have been identified that are constitutively active and antagonize the signaling between NGF and the full length TrkA (25). In contrast, the TrkB receptor, the high affinity receptor for BDNF, enhances proliferation and anchorage-independent cell growth in many cell lines (32–34) and enhances invasion in a number of cancer derived lines including neuroblastoma (9, 29, 35), colon cancer (36), head and neck squamous cell carcinoma (37), and non-small cell lung cancer (38). TrkB also enhances in vivo tumor growth in neuroblastoma (39) and transitional cell carcinoma (40). However, none of these studies have determined whether TrkB signaling in normal neural crest-derived cells is sufficient to promote an aggressive, fully transformed phenotype.

Constitutively activated TrkB in NCM-1 cells highly upregulates many genes also seen in poor prognosis neuroblastoma. *CYCLIND1* is selectively amplified in poor prognosis neuroblastoma tumors (41), as is *TWIST1*, which is expressed in 100% (7/7) of *MYCN* amplified tumors, but only 11% (2/18) of non-*MYCN* amplified tumors (42). In *MYCN* amplified neuroblastoma cell lines, *TWIST1* expression ranged from 16–164 fold that of non-*MYCN* amplified lines, levels consistent with the 39-fold increase in *twist1* expression we observe here in IgTrkB NCM-1 cells. Suggesting a specific cooperation of TWIST1 and MYCN in neuroblastoma, TWIST1 inhibits expression of the tumor suppressor P53, which allows *MYCN*-amplified tumors, and in the case of our study, IgTrkB NCM-1 cells, to escape P53-dependent apoptosis. In this study we also observed a 29-fold upregulation of *hgf* together with a 1.5-fold upregulation of the HGF receptor *c-met* in IgTrkB NCM-1

cells. Increased c-Met signaling is a common occurrence in many types of cancer (43–47), and it has also been observed in neuroblastoma (29).

IgTrkB NCM-1 cells display a greatly enhanced ability to form rapidly growing and invasive tumors compared to oncogenes expressed in other cell lines. NCM-1 cells were isolated from rat embryos and immortalized by transduction with a *v-myc*-containing replication-deficient retrovirus (22). Although *v-myc* expression itself can be transforming (48), this is not the case in NCM-1 cells because of their ability to differentiate (22), and because they do not grow in soft agar, or form tumors *in vivo*. This is confirmed by our qPCR array analysis, which showed very low, barely detectable levels of *myc* in CONT NCM-1 cells as well as in the IgTrkB NCM-1 cells. IgTrkB NCM-1 cells form large tumors prompting euthanasia of mice two weeks after a subcutaneous injection of 1 million cells; when only 100 cells are injected, 100% of the mice form tumors by 21 days. Similar *in vivo* tumor growth was seen in a *v-myc* immortalized rat fibroblast cell line expressing oncogenic BCR-ABL, however this study injected 50% more cells to initiate tumorigenesis (49). In another study, expression of the oncogene BCL2 in a rat L6 myoblast cell line expressing *v-myc* caused tumors formed only after 10 weeks (50). Recently, Schulte et. al. found JoMa1 neural crest progenitor cells (which are maintained in an undifferentiated state by inducible *c-myc* expression) can be transformed by an oncogenic variant of the ALK^{F1174L}, and 2 out of 6 mice were able to form tumors *in vivo* that were lethal to the mouse by 48 days following injection of 20 million cells (51). Thus, IgTrkB is considerably more oncogenic *in vivo* than ALK^{F1174L}. Not only did IgTrkB NCM-1 tumors grow at a rapid pace, but they are also highly invasive. In one mouse, tumor cell invasion of the spine, caused spinal cord compression, and bilateral paralysis. This spinal cord invasion mimics human neuroblastoma, where the cancer can extend into spinal foramina causing nerve root and spinal cord compression in patients with paraspinal tumors (52–54). In total, 5% of all neuroblastoma patients will present with signs related to cord impingement.

It is not clear whether the TrkB signaling is directly responsible for this transformed phenotype or if TrkB is acting through upregulation of *mycn*. Regardless, it is likely that these changes result in alterations of other genes that contribute to the aggressive phenotype of these tumors. *MYCN* amplification is the most consistent genetic alteration seen in poor prognosis neuroblastoma (55) and as evidence that *MYCN* is sufficient to drive neuroblastoma formation, the TH-*MYCN* transgenic mouse forms neuroblastoma-like tumors spontaneously (56). However, the TH-*MYCN* derived tumors are slower growing and more confined than the tumors we observed from IgTrkB NCM-1 cells. In addition, TH-*MYCN* tumors highly express BDNF, but lack TrkB expression (DeWitt and Nishi, unpublished data). JoMa1 neural crest cells overexpressing *MYCN* also form highly variable, slow growing tumors with mice surviving anywhere from 43–123 days (51). Thus, the activation of TrkB signaling likely contributes to the aggressive behavior of some tumors. On the other hand, constitutive TrkB signaling in NCM-1 cells induces a 21- fold upregulation of *mycn* mRNA in IgTrkB NCM-1 cells that is comparable to the 20- to 80-fold *MYCN* levels observed in neuroblastoma tumors and cell lines (57).

Our studies suggest that one plausible initiating event in forming aggressive neuroblastoma is the failure of TrkB expression to be down-regulated early in development. Our previous studies in showed that TrkB is transiently expressed during a developmental period when sympathoblasts are commencing differentiation and hence likely downregulating *mycn*. However, when BDNF is introduced, these TrkB positive progenitors are stimulated to divide again (7). Thus, aberrant activation of TrkB could trigger upregulation of MYCN together with the activation of additional pathways that contribute to a highly aggressive, carcinogenic phenotype. This underscores the importance of the development of therapies targeting TrkB signaling, such as lestaurtinib (CEP-701) (58).

Materials and methods

Constructs

Using a full-length rat *trkb* (WT *trkb*) construct generously provided by Dr. Moses Chao, New York University, NY, NY, we used site-directed mutagenesis to convert a single base at base pair 1814 into a *pstI* site. Both Ig-like domains could then be removed by *pstI* (New England Biolabs, Ipswich, MA) digestion due to another *pstI* site at base pair 1233. For HEK293 experiments *Igtrkb* and WT *trkb* were cloned into pcDNA3.1 (Invitrogen, San Diego, CA). For PC12 experiments *Igtrkb* was cloned into an inducible vector (pTRE-tight, Clontech, Mountain View, CA) and transfected into an rTTa-expressing PC12 Tet-on cell line (Clontech). For NCM-1 experiments *Igtrkb* was cloned into a piggyBAC transposon-transposase vector (*pmhyGENIE-3*) containing a DsRed tag and hygromycin selection gene (61). NCM-1 cells were transfected with a GFP-expressing control piggyBAC vector (*pmGENIE-3*) to establish a control cell line for in vivo experiments.

Cell Culture

Cells were grown at 37°C in 5% CO₂. HEK293 and NCM-1 cells were maintained in 10% (v/v) fetal bovine serum, 20 U/mL penicillin, 20 mg/mL streptomycin, 2mM L-glutamine, and 6 mg/mL glucose in modified L15CO₂ (62). Serum for PC12 cells was 5% fetal bovine serum and 5% heat inactivated horse serum.

Transfections

HEK293 and PC12 cells were transfected using JetPEI (Polyplus transfection, Illkirch, France). Stably transfected HEK293 cells were established by G418 (Sigma, St. Louis, MO) selection. NCM-1 cells were transfected using X-tremeGENE 9 (Roche, Indianapolis, IN) and stable cells were established by hygromycin (Sigma) selection.

Westerns

Cells were seeded at 250,000 per well in 6-well plates. For HEK293 experiments cells were serum starved for 24 hours, treated with, or without BDNF (100ng/mL, R&D Systems) for 1 hour and then collected for SDS PAGE by direct lysis into 100μL 1x SDS sample buffer+β-Mercaptoethanol (βMe). Samples were run on an 8% polyacrylamide gel, then transferred to a nitrocellulose membrane (Osmonics, Inc., Minnetonka, MN) overnight at 4°C at 30 volts (Hoefer Scientific Instruments, San Francisco, CA). Blots were incubated with primary antibodies overnight at 4°C followed by appropriate secondary antibodies for 1 hour at room

temperature. Primary antibodies used were: goat anti-TrkB (1:1000, R&D Systems); rabbit anti-p-Erk1/2 (1:500, Cell Signaling, Boston, MA); goat anti- β actin (1:1000, Santa Cruz, Santa Cruz, CA); rabbit anti-Phospho-Histone H3 (1:500, Cell Signaling); and mouse anti-Cyclin D1 (1:1000; Cell Signaling). Secondary antibodies used were donkey anti-goat 700 (Rockland, Gilbertsville, PA); donkey anti-rabbit 800 (Rockland); and donkey anti-mouse 800 (Rockland) all at 1:10 000. Blots were analyzed using an Odyssey Infrared Imager (LI-COR Biosciences, Lincoln, NE).

PC12 neurite outgrowth

PC12 cells were plated on poly-D-lysine (0.5 mg/mL, Sigma) and laminin (0.02 mg/mL, purified in the Nishi lab from EHS tumors grown subcutaneously in C57Bl6 mice) coated coverslips at 50,000 cells per well. The day after plating, cells were transfected with either an inducible GFP or the inducible *Igtrkb* construct and allowed to recover for 48 hrs prior to treatment with doxycycline (1 μ g/mL, Sigma) and 7s NGF (1 μ g/mL, Alomone, Jerusalem, Israel). Coverslips were fixed 30 min in Zamboni's fixative (4% (w/v) paraformaldehyde, 15% (v/v) picric acid in 0.1 M sodium phosphate buffer, pH 7.4) and processed for immunocytochemistry as previously described (63). Primary antibodies were: goat anti-TrkB (1:1000, R&D Systems); chicken anti-GFP (1:1000, Aves, Tigard, OR). Secondary antibodies were: donkey anti-goat alexa 488 (1:1000, Invitrogen) and goat anti-chicken alexa 488 (1:1000, Invitrogen). A Nikon Eclipse E800 microscope connected to a computer equipped with StereoInvestigator software (MBF Bioscience, Williston, VT) was used to count neurite positive PC12 cells (at least one process of a length at least twice the cell's soma size).

Calcein AM

NCM-1 cells were plated on poly-D-lysine coated 96 well plates at 200 cells per well in 100 μ L of media and viability assessed using 2 μ M calcein AM (Molecular Probes, Eugene, OR) with a FLUOstar Galaxy (BMG, Cary, NC) fluorescent microplate reader. Each condition was replicated in a minimum of 8 wells on the same plate. For K252a (Merck, Darmstadt, Germany) and c-Met inhibitor (SU11274, Merck) experiments, inhibitors (50 nM and 1 μ m, respectively) were added at the time of plating.

Soft agar assay

6-well plates were coated with 0.5% agar (Affymetrix, Santa Clara, CA) in growth medium. After this base layer had solidified, NCM-1 cells suspended in 0.35% agar were plated on top of the base layer at 1000 cells per well. Cells were fed by adding 0.5mL of media to the top of each well every 3 days. After 10 days, cultures were fixed overnight with 4% paraformaldehyde in PBS, then stained with 0.005% crystal violet.

Anoikis assay

To quantify anoikis, medium was collected 3 days after cultures achieved confluence and the number of live cells growing in the media was quantified by trypan blue (0.08%, Sigma) exclusion and a hemocytometer.

Migration and invasion

The 'donut assay' for migration and invasion was used as described (28). 10,000 cells were plated on poly-D-lysine and laminin coated coverslips in a 10 μ L volume. Initial images were acquired through a 2X PlanApo objective on a Nikon Eclipse TE-2000E inverted microscope. A second set of images acquired at 24 hours were compared and analyzed using the default settings of a custom written ImageJ macro. Area migrated/invaded was quantified by measuring the area between the outer bound of the farthest migrating/invading cells after 24 hours, and the bound of the cells directly after gasket removal.

RNA extraction and qPCR array

Cells were grown to confluence in 6-well plates, lysed directly into TRI Reagent (Molecular Research Center, Cincinnati, OH), and RNA was isolated using the manufacturer's protocol. RNA quality and genomic DNA contamination were assessed using an Agilent 2100 Bioanalyzer (Agilent Technologies, Santa Clara, CA). Reverse transcription and Cancer Pathways qPCR array plate (SABiosciences, Valencia, CA) analysis were performed at the UVM Vermont Cancer Center DNA Analysis Facility using RT² First Strand kit (SABiosciences, Valencia, CA). Data shown in Tables 1 and 2 represent the mean of three independently isolated RNA samples from 3 different wells of a 6 well plate for each cell line. *Mycn* expression transcription levels were evaluated by reverse transcription of 1 μ g of RNA transcribed to cDNA using (Superscript III, Invitrogen) and subsequent Taqman-based qPCR (ABI).

In vivo

Mice were housed in an NIH and AALAC approved animal facility at UVM and treated following an approved IACUC protocol. Cells were injected subcutaneously into flanks of NOD-SCID mice at 10⁶ cells per mouse in 200 μ L of matrigel (BD Biosciences). Four mice injected per cell line. When tumors became palpable, tumor growth was quantified every other day at first, and then daily when it became apparent TrkB tumors were fast growing. Tumor volume estimated from length and width measurements using the established formula $v=1.58(\pi/6)(L*W)^{(3/2)}$ (59). To examine the lower limits of the tumorigenic potential of IgTrkB NCM-1 cells, 100 cells in 200 μ L of matrigel were injected into 3 NOD-SCID mice, which were monitored for tumor formation.

Supplementary Material

Refer to Web version on PubMed Central for supplementary material.

Acknowledgments

The authors would like to thank Felix Eckenstein, Andy McKenzie, and Nourine Ahmed for technical assistance. We also thank Alan Howe for helpful comments on our manuscript and for assistance with the "donut" assay. Portions of this work were performed in the DNA Analysis Facility at the Vermont Cancer Center and the Neuroscience COBRE Molecular Cellular Core at the University of Vermont. This work was funded by Alex's Lemonade Foundation (RN); R21NS25788 (RN); P30RR032135 (COBRE); P30GM103498 (COBRE); 5P20RR024206 (SM); and R01GM083158-01A1 (SM).

References

1. Maris JM, Hogarty MD, Bagatell R, Cohn SL. Neuroblastoma. *Lancet*. 2007 Jun 23; 369(9579): 2106–20. [PubMed: 17586306]
2. Brodeur GM. Neuroblastoma: biological insights into a clinical enigma. *Nat Rev Cancer*. 2003 Mar; 3(3):203–16. [PubMed: 12612655]
3. Miller FD, Kaplan DR. Neurotrophin signalling pathways regulating neuronal apoptosis. *Cell Mol Life Sci*. 2001 Jul; 58(8):1045–53. [PubMed: 11529497]
4. Reichardt LF. Neurotrophin-regulated signalling pathways. *Philos Trans R Soc Lond B Biol Sci*. 2006 Sep 29; 361(1473):1545–64. [PubMed: 16939974]
5. Nakagawara A. Molecular basis of spontaneous regression of neuroblastoma: role of neurotrophic signals and genetic abnormalities. *Hum Cell*. 1998 Sep; 11(3):115–24. [PubMed: 10086274]
6. Schramm A, Schulte JH, Astrahantseff K, Apostolov O, Limpt V, Sieverts H, et al. Biological effects of TrkA and TrkB receptor signaling in neuroblastoma. *Cancer Lett*. 2005 Oct 18; 228(1–2): 143–53. [PubMed: 15921851]
7. Straub JA, Sholler GL, Nishi R. Embryonic sympathoblasts transiently express TrkB in vivo and proliferate in response to brain-derived neurotrophic factor in vitro. *BMC Dev Biol*. 2007; 7:10. [PubMed: 17309801]
8. Reiff T, Tsarovina K, Majdzari A, Schmidt M, del Pino I, Rohrer H. Neuroblastoma phox2b variants stimulate proliferation and dedifferentiation of immature sympathetic neurons. *J Neurosci*. Jan 20; 30(3):905–15. [PubMed: 20089899]
9. Matsumoto K, Wada RK, Yamashiro JM, Kaplan DR, Thiele CJ. Expression of brain-derived neurotrophic factor and p145TrkB affects survival, differentiation, and invasiveness of human neuroblastoma cells. *Cancer Res*. 1995 Apr 15; 55(8):1798–806. [PubMed: 7712490]
10. Brodeur GM, Nakagawara A, Yamashiro DJ, Ikegaki N, Liu XG, Azar CG, et al. Expression of TrkA, TrkB and TrkC in human neuroblastomas. *J Neurooncol*. 1997 Jan; 31(1–2):49–55. [PubMed: 9049830]
11. Nakagawara A, Azar CG, Scavarda NJ, Brodeur GM. Expression and function of TRK-B and BDNF in human neuroblastomas. *Mol Cell Biol*. 1994 Jan; 14(1):759–67. [PubMed: 8264643]
12. Kim CJ, Matsuo T, Lee KH, Thiele CJ. Up-regulation of insulin-like growth factor-II expression is a feature of TrkA but not TrkB activation in SH-SY5Y neuroblastoma cells. *Am J Pathol*. 1999 Nov; 155(5):1661–70. [PubMed: 10550322]
13. Scala S, Wosikowski K, Giannakakou P, Valle P, Biedler JL, Spengler BA, et al. Brain-derived neurotrophic factor protects neuroblastoma cells from vinblastine toxicity. *Cancer Res*. 1996 Aug 15; 56(16):3737–42. [PubMed: 8706017]
14. Jaboin J, Kim CJ, Kaplan DR, Thiele CJ. Brain-derived neurotrophic factor activation of TrkB protects neuroblastoma cells from chemotherapy-induced apoptosis via phosphatidylinositol 3'-kinase pathway. *Cancer Res*. 2002 Nov 15; 62(22):6756–63. [PubMed: 12438277]
15. Ho R, Eggert A, Hishiki T, Minturn JE, Ikegaki N, Foster P, et al. Resistance to chemotherapy mediated by TrkB in neuroblastomas. *Cancer Res*. 2002 Nov 15; 62(22):6462–6. [PubMed: 12438236]
16. Eggert A, Grotzer MA, Ikegaki N, Liu XG, Evans AE, Brodeur GM. Expression of the neurotrophin receptor TrkA down-regulates expression and function of angiogenic stimulators in SH-SY5Y neuroblastoma cells. *Cancer Res*. 2002 Mar 15; 62(6):1802–8. [PubMed: 11912158]
17. Nakamura K, Martin KC, Jackson JK, Beppu K, Woo CW, Thiele CJ. Brain-derived neurotrophic factor activation of TrkB induces vascular endothelial growth factor expression via hypoxia-inducible factor-1alpha in neuroblastoma cells. *Cancer Res*. 2006 Apr 15; 66(8):4249–55. [PubMed: 16618748]
18. Arevalo JC, Conde B, Hempstead BL, Chao MV, Martin-Zanca D, Perez P. TrkA immunoglobulin-like ligand binding domains inhibit spontaneous activation of the receptor. *Mol Cell Biol*. 2000 Aug; 20(16):5908–16. [PubMed: 10913174]
19. Greene LA, Tischler AS. Establishment of a noradrenergic clonal line of rat adrenal pheochromocytoma cells which respond to nerve growth factor. *Proc Natl Acad Sci U S A*. 1976 Jul; 73(7):2424–8. [PubMed: 1065897]

20. Kaplan DR, Martin-Zanca D, Parada LF. Tyrosine phosphorylation and tyrosine kinase activity of the *trk* proto-oncogene product induced by NGF. *Nature*. 1991 Mar 14; 350(6314):158–60. [PubMed: 1706478]
21. Jian Z, Nonaka I, Hattori S, Nakamura S. Activation of Ras and protection from apoptotic cell death by BDNF in PC12 cells expressing TrkB. *Cell Signal*. 1996 Aug; 8(5):365–70. [PubMed: 8911685]
22. Lo LC, Birren SJ, Anderson DJ. V-myc immortalization of early rat neural crest cells yields a clonal cell line which generates both glial and adrenergic progenitor cells. *Dev Biol*. 1991 May; 145(1):139–53. [PubMed: 1673438]
23. Urschitz J, Kawasumi M, Owens J, Morozumi K, Yamashiro H, Stoytchev I, et al. Helper-independent piggyBac plasmids for gene delivery approaches: strategies for avoiding potential genotoxic effects. *Proc Natl Acad Sci U S A*. 2010 May 4; 107(18):8117–22. [PubMed: 20404201]
24. Singh RK, Lange TS, Kim K, Zou Y, Lieb C, Sholler GL, et al. Effect of indole ethyl isothiocyanates on proliferation, apoptosis, and MAPK signaling in neuroblastoma cell lines. *Bioorg Med Chem Lett*. 2007 Nov 1; 17(21):5846–52. [PubMed: 17855093]
25. Tacconelli A, Farina AR, Cappabianca L, Desantis G, Tessitore A, Vetusch A, et al. TrkA alternative splicing: a regulated tumor-promoting switch in human neuroblastoma. *Cancer Cell*. 2004 Oct; 6(4):347–60. [PubMed: 15488758]
26. Thullberg M, Stromblad S. Anchorage-independent cytokinesis as part of oncogenic transformation? *Cell Cycle*. 2008 Apr 15; 7(8):984–8. [PubMed: 18414025]
27. Chiarugi P, Giannoni E. Anoikis: a necessary death program for anchorage-dependent cells. *Biochem Pharmacol*. 2008 Dec 1; 76(11):1352–64. [PubMed: 18708031]
28. McKenzie AJ, Campbell SL, Howe AK. Protein kinase A activity and anchoring are required for ovarian cancer cell migration and invasion. *PLoS One*. 6(10):e26552. [PubMed: 22028904]
29. Hecht M, Schulte JH, Eggert A, Wilting J, Schweigerer L. The neurotrophin receptor TrkB cooperates with c-Met in enhancing neuroblastoma invasiveness. *Carcinogenesis*. 2005 Dec; 26(12):2105–15. [PubMed: 16051641]
30. Li CW, Xia W, Huo L, Lim SO, Wu Y, Hsu JL, et al. Epithelial-Mesenchymal Transition Induced by TNF-alpha Requires NF-kappaB-Mediated Transcriptional Upregulation of Twist1. *Cancer Res*. 2012 Mar 1; 72(5):1290–300. [PubMed: 22253230]
31. Martin-Zanca D, Hughes SH, Barbacid M. A human oncogene formed by the fusion of truncated tropomyosin and protein tyrosine kinase sequences. *Nature*. 1986 Feb-Mar; 319(6056):743–8. [PubMed: 2869410]
32. Douma S, Van Laar T, Zevenhoven J, Meuwissen R, Van Garderen E, Peeper DS. Suppression of anoikis and induction of metastasis by the neurotrophic receptor TrkB. *Nature*. 2004 Aug 26; 430(7003):1034–9. [PubMed: 15329723]
33. Glass DJ, Nye SH, Hantzopoulos P, Macchi MJ, Squinto SP, Goldfarb M, et al. TrkB mediates BDNF/NT-3-dependent survival and proliferation in fibroblasts lacking the low affinity NGF receptor. *Cell*. 1991 Jul 26; 66(2):405–13. [PubMed: 1649703]
34. Klein R, Nanduri V, Jing SA, Lamballe F, Tapley P, Bryant S, et al. The *trkB* tyrosine protein kinase is a receptor for brain-derived neurotrophic factor and neurotrophin-3. *Cell*. 1991 Jul 26; 66(2):395–403. [PubMed: 1649702]
35. Cimmino F, Schulte JH, Zollo M, Koster J, Versteeg R, Iolascon A, et al. Galectin-1 is a major effector of TrkB-mediated neuroblastoma aggressiveness. *Oncogene*. 2009 May 14; 28(19):2015–23. [PubMed: 19363525]
36. Yu Y, Zhang S, Wang X, Yang Z, Ou G. Overexpression of TrkB promotes the progression of colon cancer. *APMIS*. 2010 Mar; 118(3):188–95. [PubMed: 20132184]
37. Kupferman ME, Jiffar T, El-Naggar A, Yilmaz T, Zhou G, Xie T, et al. TrkB induces EMT and has a key role in invasion of head and neck squamous cell carcinoma. *Oncogene*. Apr 8; 29(14):2047–59. [PubMed: 20101235]
38. Zhang S, Guo D, Luo W, Zhang Q, Zhang Y, Li C, et al. TrkB is highly expressed in NSCLC and mediates BDNF-induced the activation of Pyk2 signaling and the invasion of A549 cells. *BMC Cancer*. 2010; 10:43. [PubMed: 20156366]

39. Brodeur GM, Minturn JE, Ho R, Simpson AM, Iyer R, Varela CR, et al. Trk receptor expression and inhibition in neuroblastomas. *Clin Cancer Res.* 2009 May 15; 15(10):3244–50. [PubMed: 19417027]
40. Huang YT, Lai PC, Wu CC, Hsu SH, Cheng CC, Lan YF, et al. BDNF mediated TrkB activation is a survival signal for transitional cell carcinoma cells. *Int J Oncol.* 2010 Jun; 36(6):1469–76. [PubMed: 20428771]
41. Molenaar JJ, Koster J, Ebus ME, van Sluis P, Westerhout EM, de Preter K, et al. Copy number defects of G1-cell cycle genes in neuroblastoma are frequent and correlate with high expression of E2F target genes and a poor prognosis. *Genes Chromosomes Cancer.* 2011 Jan; 51(1):10–9. [PubMed: 22034077]
42. Valsesia-Wittmann S, Magdeleine M, Dupasquier S, Garin E, Jallas AC, Combaret V, et al. Oncogenic cooperation between H-Twist and N-Myc overrides failsafe programs in cancer cells. *Cancer Cell.* 2004 Dec; 6(6):625–30. [PubMed: 15607966]
43. Liu C, Park M, Tsao MS. Overexpression of c-met proto-oncogene but not epidermal growth factor receptor or c-erbB-2 in primary human colorectal carcinomas. *Oncogene.* 1992 Jan; 7(1):181–5. [PubMed: 1741162]
44. Tokunou M, Niki T, Eguchi K, Iba S, Tsuda H, Yamada T, et al. c-MET expression in myofibroblasts: role in autocrine activation and prognostic significance in lung adenocarcinoma. *Am J Pathol.* 2001 Apr; 158(4):1451–63. [PubMed: 11290563]
45. Lengyel E, Prechtel D, Resau JH, Gauger K, Welk A, Lindemann K, et al. C-Met overexpression in node-positive breast cancer identifies patients with poor clinical outcome independent of Her2/neu. *Int J Cancer.* 2005 Feb 10; 113(4):678–82. [PubMed: 15455388]
46. Ramirez R, Hsu D, Patel A, Fenton C, Dinauer C, Tuttle RM, et al. Over-expression of hepatocyte growth factor/scatter factor (HGF/SF) and the HGF/SF receptor (cMET) are associated with a high risk of metastasis and recurrence for children and young adults with papillary thyroid carcinoma. *Clin Endocrinol (Oxf).* 2000 Nov; 53(5):635–44. [PubMed: 11106926]
47. Furukawa T, Duguid WP, Kobari M, Matsuno S, Tsao MS. Hepatocyte growth factor and Met receptor expression in human pancreatic carcinogenesis. *Am J Pathol.* 1995 Oct; 147(4):889–95. [PubMed: 7573364]
48. Ramsay GM, Moscovici G, Moscovici C, Bishop JM. Neoplastic transformation and tumorigenesis by the human protooncogene MYC. *Proc Natl Acad Sci U S A.* 1990 Mar; 87(6):2102–6. [PubMed: 2156260]
49. Lugo TG, Witte ON. The BCR-ABL oncogene transforms Rat-1 cells and cooperates with v-myc. *Mol Cell Biol.* 1989 Mar; 9(3):1263–70. [PubMed: 2725497]
50. Screaton RA, Penn LZ, Stanners CP. Carcinoembryonic antigen, a human tumor marker, cooperates with Myc and Bcl-2 in cellular transformation. *J Cell Biol.* 1997 May 19; 137(4):939–52. [PubMed: 9151695]
51. Schulte JH, Lindner S, Bohrer A, Maurer J, De Preter K, Lefever S, et al. MYCN and ALKF1174L are sufficient to drive neuroblastoma development from neural crest progenitor cells. *Oncogene.* 2012 Apr 9.
52. De Bernardi B, Pianca C, Pistamiglio P, Veneselli E, Viscardi E, Pession A, et al. Neuroblastoma with symptomatic spinal cord compression at diagnosis: treatment and results with 76 cases. *J Clin Oncol.* 2001 Jan 1; 19(1):183–90. [PubMed: 11134211]
53. De Bernardi B, Balwierz W, Bejent J, Cohn SL, Garre ML, Iehara T, et al. Epidural compression in neuroblastoma: Diagnostic and therapeutic aspects. *Cancer Lett.* 2005 Oct 18; 228(1–2):283–99. [PubMed: 15975710]
54. Plantaz D, Rubie H, Michon J, Mechinaud F, Coze C, Chastagner P, et al. The treatment of neuroblastoma with intraspinal extension with chemotherapy followed by surgical removal of residual disease. A prospective study of 42 patients--results of the NBL 90 Study of the French Society of Pediatric Oncology. *Cancer.* 1996 Jul 15; 78(2):311–9. [PubMed: 8674009]
55. Seeger RC, Brodeur GM, Sather H, Dalton A, Siegel SE, Wong KY, et al. Association of multiple copies of the N-myc oncogene with rapid progression of neuroblastomas. *N Engl J Med.* 1985 Oct 31; 313(18):1111–6. [PubMed: 4047115]

56. Weiss WA, Aldape K, Mohapatra G, Feuerstein BG, Bishop JM. Targeted expression of MYCN causes neuroblastoma in transgenic mice. *EMBO J.* 1997 Jun 2; 16(11):2985–95. [PubMed: 9214616]
57. Schwab M, Ellison J, Busch M, Rosenau W, Varmus HE, Bishop JM. Enhanced expression of the human gene N-myc consequent to amplification of DNA may contribute to malignant progression of neuroblastoma. *Proc Natl Acad Sci U S A.* 1984 Aug; 81(15):4940–4. [PubMed: 6589638]
58. Minturn JE, Evans AE, Villablanca JG, Yanik GA, Park JR, Shusterman S, et al. Phase I trial of lestaurtinib for children with refractory neuroblastoma: a new approaches to neuroblastoma therapy consortium study. *Cancer Chemother Pharmacol.* 2011 Oct; 68(4):1057–65. [PubMed: 21340605]
59. Feldman JP, Goldwasser R, Mark S, Schwartz J, Orion I. A mathematical model for tumor volume evaluation using two dimensions. *Journal of Applied Quantitative Methods.* 2009; 4(4):455–62.

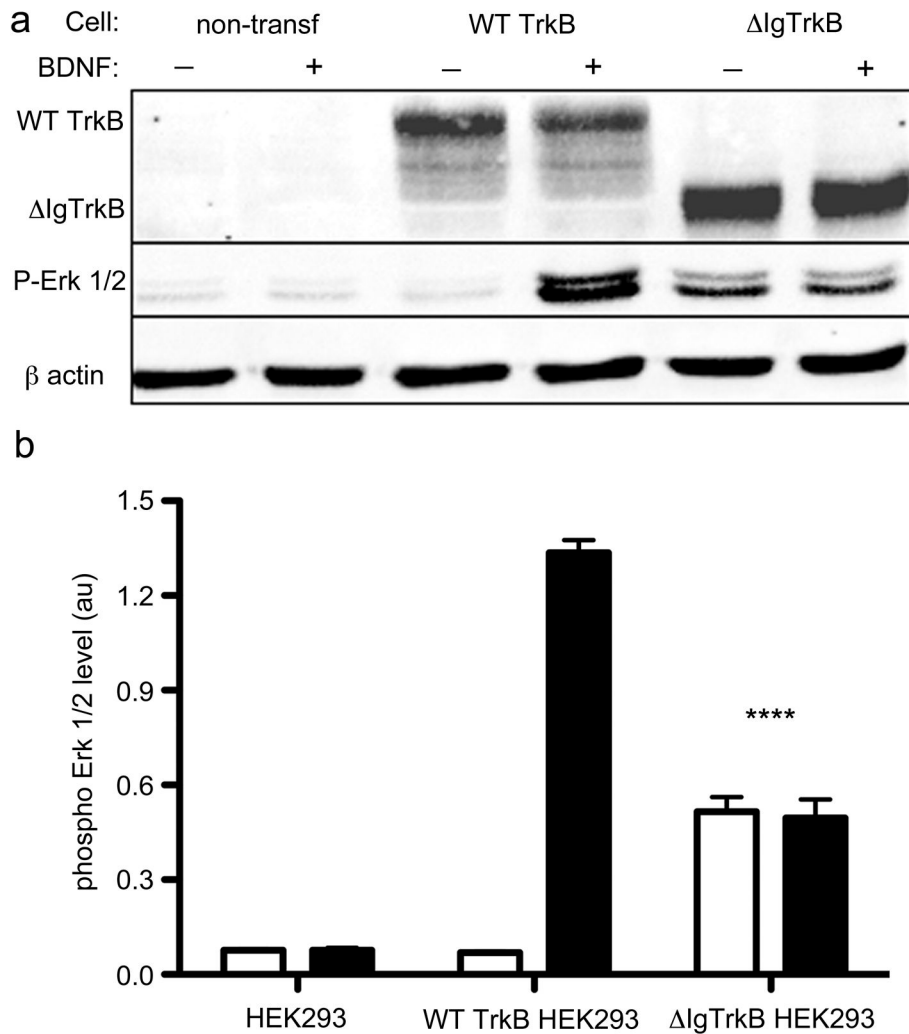


Figure 1.

IgTrkB is expressed and is constitutively active. HEK293 cells were stably transfected with either a WT or IgTrkB construct. Cells were then treated with or without BDNF (100 ng/mL) and protein was isolated. **(a)** Western blot for TrkB and phosphorylated Erk 1/2 demonstrates that IgTrkB is expressed, and signals in the absence of the TrkB ligand BDNF. **(b)** Quantification of phosphorylated Erk 1/2 protein expression reveals a significant increase in phospho Erk 1/2 in IgTrkB transfected cells treated with (black bars), or without (white bars) BDNF, compared to untreated WT TrkB transfected cells ($p < 0.0001$, ANOVA, $n=3$, error bars = SEM) or untransfected HEK293 cells. Constitutive IgTrkB activity is two-fifths that of the WT TrkB receptor treated with BDNF.

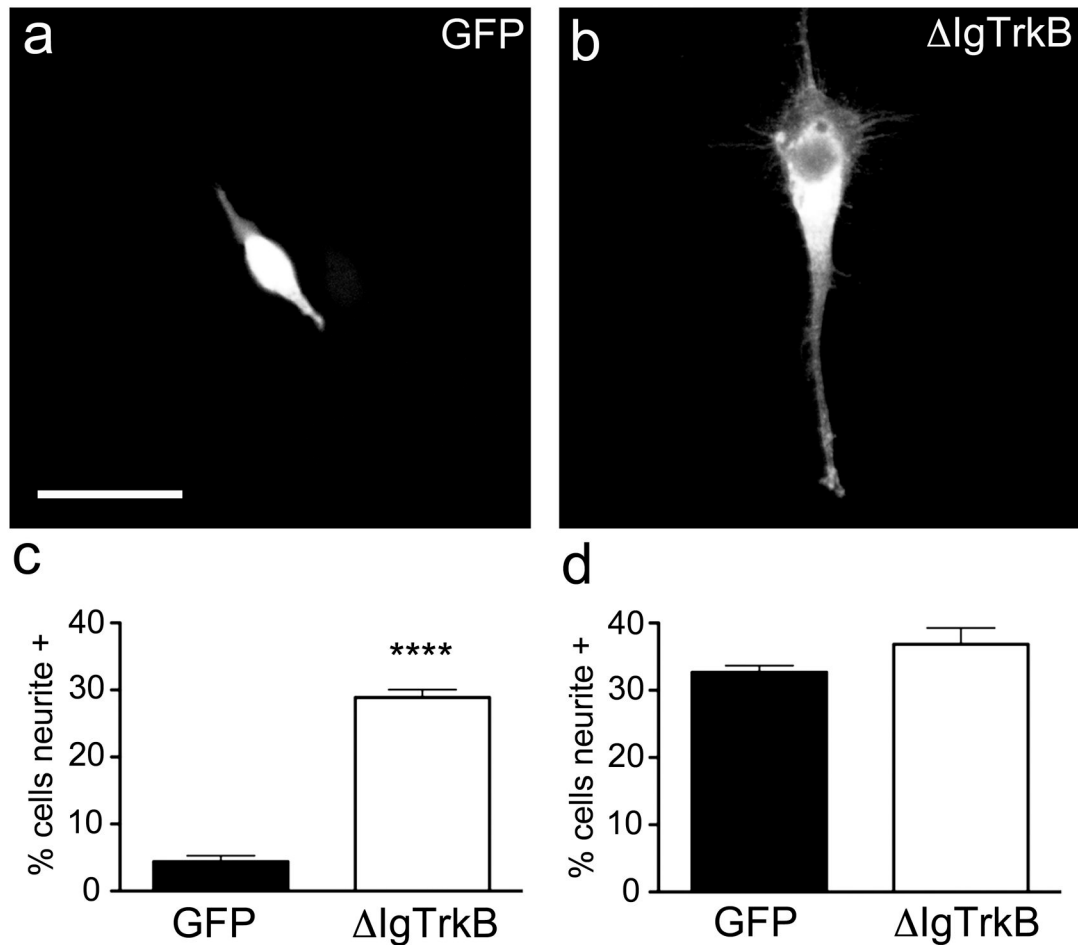


Figure 2.

IgTrkB promotes process outgrowth in PC12 cells. Transfected cells were assessed for process outgrowth 6 days following transfection. (a) PC12 cells transfected with GFP have minimal neurite outgrowth, (b) while Δ IgTrkB transfection stimulates neurite outgrowth. (c) Quantification of process outgrowth in PC12 cells reveals a 6-fold increase in the number of cells bearing neurites when transfected with Δ IgTrkB as opposed to a GFP control plasmid ($p < 0.0001$, Student's t-test, $n=3$, error bars = SEM). (d) In the presence of NGF the number of cells bearing neurites is equivalent in the two transfection conditions. Scale bar is equivalent to 25 μ m and applies to both images.

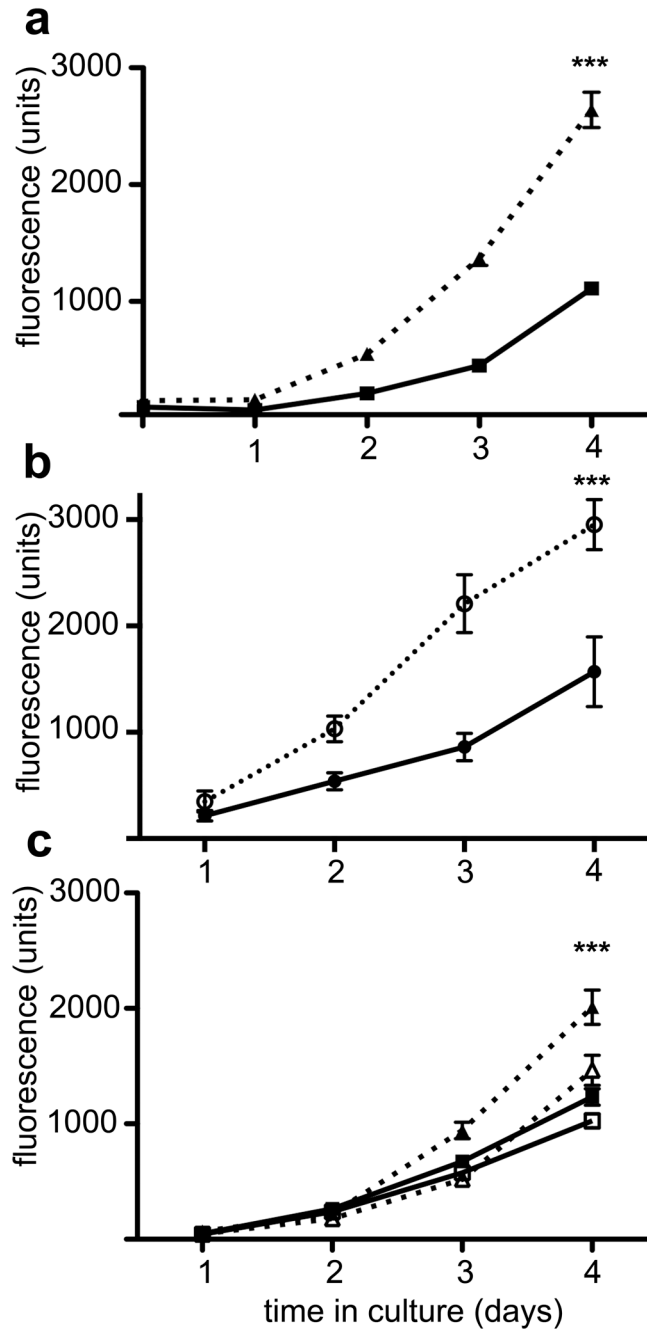


Figure 3.

IgTrkB and full length TrkB promote proliferation in the neural crest derived cell line NCM-1. Cultures in 96 well plates were seeded with the same number of cells on day 0, then grown for the indicated periods of time up to 4 days and the number of cells were quantified using Calcein AM uptake. **(a)** stably transfected IgTrkB NCM-1 cells (closed triangles) grow faster than the parent CONT NCM-1 cell line (closed squares; $p < 0.0001$, ANOVA; $n=16$). **(b)** full length TrkB expressing cells exhibit an enhanced rate with BDNF (open circles) over the same cell line grown in the absence of BDNF (closed circles; $p < 0.0001$,

ANOVA, n=8) (c) The pan-Trk inhibitor K252a (50 nM) abolishes increased proliferation ($p < 0.0001$, ANOVA, n=8, error bars = SEM) in IgTrkB NCM-1 cells (open triangles) compared to DMSO treated IgTrkB NCM-1 cells (closed triangles). IgTrkB proliferation in the presence of K252a is similar to WT NCM-1 proliferation in the presence of either K252a (open squares) or DMSO (closed squares).

Author Manuscript

Author Manuscript

Author Manuscript

Author Manuscript

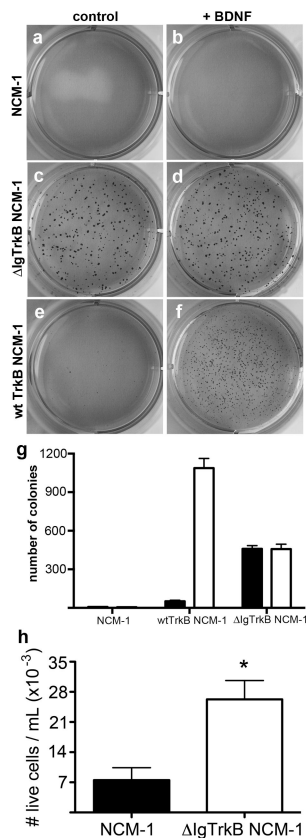


Figure 4.

IgTrkB promotes anchorage-independent cell growth and anoikis resistance in NCM-1 cells. **(a, b)** The CONT NCM-1 cells have little ability to grow in soft agar, even when BDNF is added **(b)**. **(c,d)** IgTrkB NCM-1 cells form numerous colonies even in the absence of BDNF **(c)**. **(e,f)** NCM-1 cells stably transfected with WT TrkB form colonies only when BDNF is added **(f)**. **(g)** Quantification of cultures shown in **a–f** ($p < 0.001$, Student's t-test, $n=6$, error bars = SEM). **(h)** IgTrkB NCM-1 cells are also resistant to detachment-induced apoptosis marked by a significant increase ($p < 0.05$, Student's t-test, $n=4$, error bars = SEM) in the number of live cells in suspension as determined by trypan blue exclusion from media taken from confluent cultures.

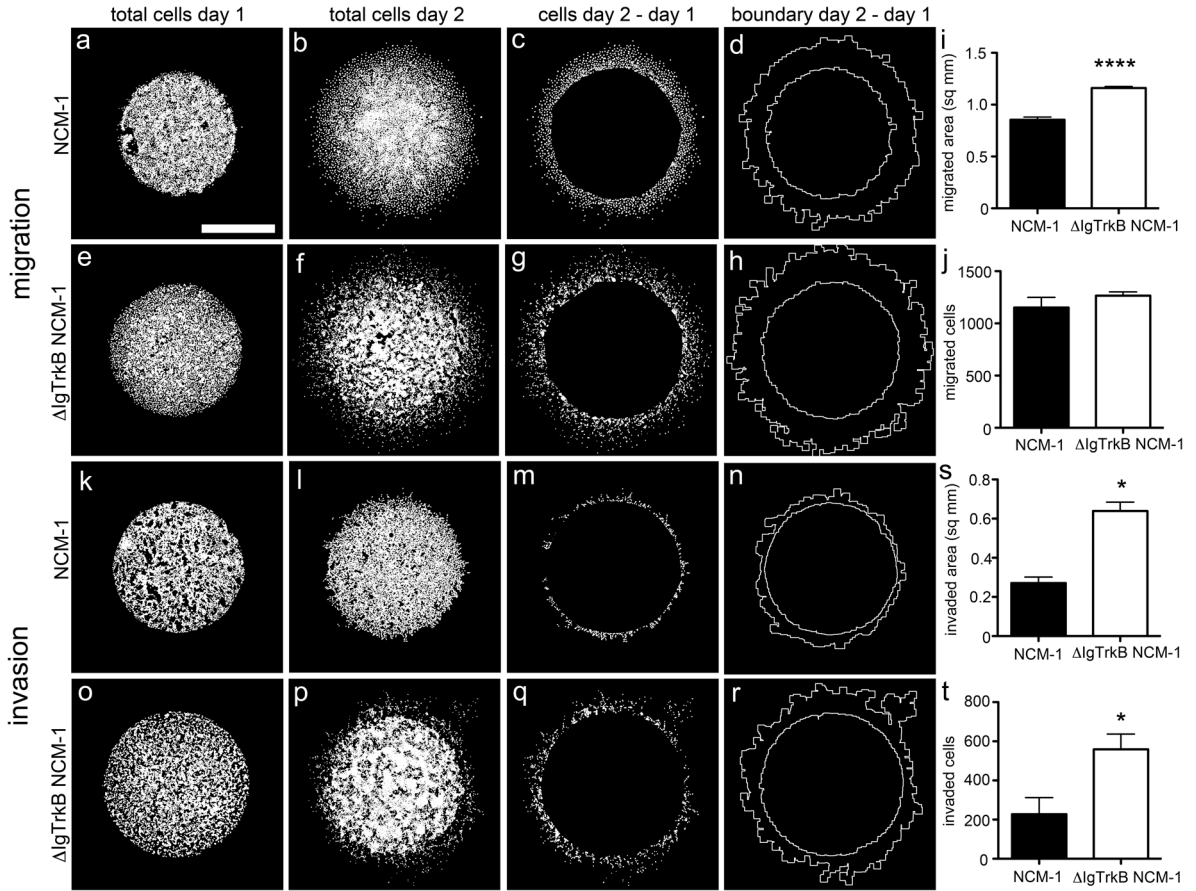


Figure 5.

IgTrkB enhances migration and invasion of NCM-1 cells in donut migration assay. **(a–d)** Migration in CONT NCM-1 and **(e–h)** IgTrkB NCM-1 cells. **(i)** Quantification of migration shows a significant increase in the area migrated ($p < 0.0001$, Student's t-test, $n=8$, error bars = SEM) in IgTrkB NCM-1 cells **(h)** compared to **(d)**, **(j)** but no difference in the total number of cells migrated. For invasion assay, cells were overlaid with matrigel. **(k–n)** Matrigel invasion in CONT NCM-1 and **(o–r)** IgTrkB NCM-1 cells. **(s)** IgTrkB significantly enhances both area invaded **(r)** compared to **(n)**, and **(t)** the total number of invading NCM-1 cells ($p < 0.05$, Student's t-test, $n=3$, error bars = SEM). Scale bar is equivalent to 1mm and applies to all panels.

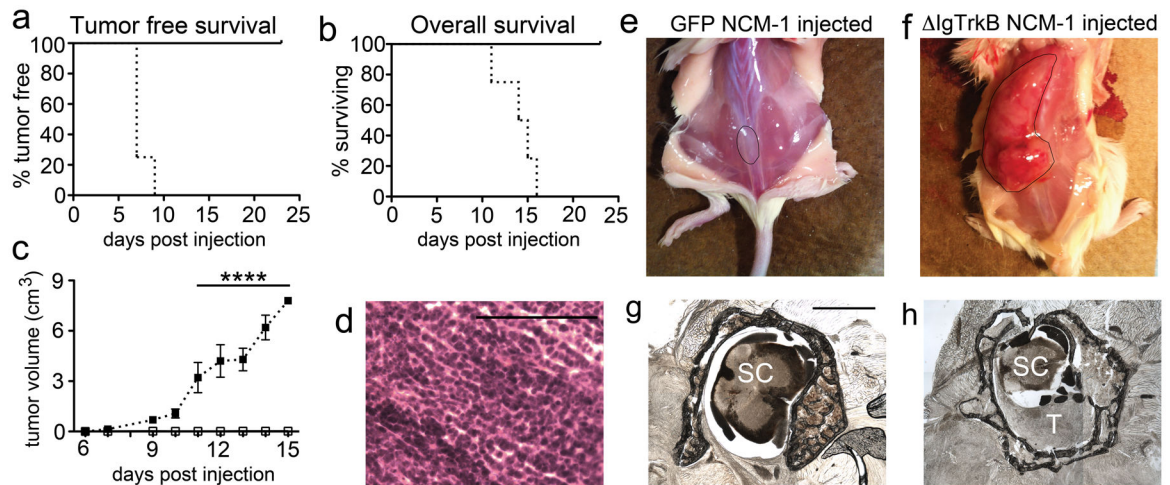


Figure 6.

IgTrkB NCM-1 cells form highly aggressive tumors in vivo. **(a)** Kaplan-Meier plot of tumor free survival in NOD-SCID mice subcutaneously injected with GFP NCM-1 cells (solid line), or IgTrkB NCM-1 cells (dotted line). No mice injected with GFP NCM-1 cells formed tumors over the course of the experiment ($p < 0.01$, log-rank (Mantel-Cox) test, $n=4$). **(b)** Kaplan-Meier plot of overall survival. All IgTrkB NCM-1 cell injected mice had to be sacrificed by 15 days after initial cell injection due to tumor burden ($p < 0.01$, log-rank (Mantel-Cox) test, $n=4$). **(c)** Estimated tumor volume over the course of the experiment.

IgTrkB NCM-1 cell injected mice formed rapidly growing tumors starting at 1 week following initial cell injection, with a significant difference in tumor volume versus matrigel plug volume by 11 days ($p < 0.0001$, ANOVA, $n=4$, error bars = SEM). Removed tumors had an average wet weight of 4.5 grams. **(d)** Hematoxylin and Eosin staining of tumor tissue reveals densely packed cells with scant cytoplasm and absent extracellular stroma reminiscent of poor prognosis neuroblastoma. **(e)** Example of mouse injected with GFP NCM-1 cells, and **(f)** IgTrkB NCM-1 cells (matrigel **(e)** and tumor **(f)** are outlined in black). **(g-h)** In one mouse, the tumor invaded the spinal cord causing bilateral hind limb paralysis. **(g)** Normal thoracic spinal cord (labeled SC) surrounded by vertebrae, rostral to tumor invasion. **(h)** The lower thoracic spinal cord (labeled SC) is compressed in the vertebrae by invading tumor cells (labeled T). Scale bar in **(g)** is equivalent to 1mm and also applies to **(h)**. Scale bar in **(d)** is equivalent to 100 μm .

Table 1

Tumor promoters upregulated in IgTrkB NCM-1 cells

Symbol	Gene	Fold Regulation	P-value	Description
<i>ccnd1</i>	Cyclin D1	436.1	0.000069	Promotes cell cycle progression
<i>twist1</i>	Twist homolog 1 (Drosophila)	38.57	0.000015	Promotes epithelial- mesenchymal transition (EMT), invasion, and metastasis
<i>hgf</i>	Hepatocyte growth factor	28.86	0.008818	Promotes mitogenesis, cell motility, and matrix invasion
<i>ccnd2</i>	Cyclin D2	26.40	0.000137	Promotes cell cycle progression
<i>fgf2</i>	Fibroblast growth factor 2	19.88	0.001753	Promotes angiogenesis
<i>angpt1</i>	Angiopoietin 1	12.25	0.003952	Promotes angiogenesis
<i>abcg2</i>	ATP-binding cassette, subfamily G (WHITE), member 2	6.385	0.000792	Mediates multidrug resistance
<i>mucl</i>	Mucin 1, cell surface associated	4.884	0.000030	Inhibits p53-mediated apoptosis, and promotes EMT through β -catenin stabilization
<i>vegfa</i>	Vascular endothelial growth factor A	4.816	0.000115	Promotes angiogenesis
<i>serpine1</i>	Serpin peptidase inhibitor, clade E (nexin, plasminogen activator inhibitor type 1), member 1	4.661	0.000027	Promotes invasion and metastasis

Table 2

Tumor suppressors downregulated in IgTrkB NCM-1 cells

Symbol	Gene	Fold Regulation	P-value	Description
<i>thbs1</i>	Thrombospondin 1	-2.118	0.000563	Promotes cell adhesion
<i>pik3r1</i>	Phosphoinositide-3-kinase, regulatory subunit 1 (alpha)	-1.913	0.000261	Inhibitor of PI3K signaling
<i>rb1</i>	Retinoblastoma 1	-1.771	0.000464	Inhibits cell cycle progression
<i>tgfb1</i>	Transforming growth factor, beta receptor 1	-1.755	0.001248	Inhibits cell growth
<i>pten</i>	Phosphatase and tensin homolog	-1.710	0.000285	Inhibits cell proliferation
<i>bad</i>	BCL2-associated agonist of cell death	-1.572	0.004340	Promotes apoptosis
<i>cdkn1a</i>	Cyclin-dependent kinase inhibitor 1A	-1.514	0.000064	Inhibits cell cycle progression

Author Manuscript

Author Manuscript

Author Manuscript

Author Manuscript